

Experimental study on the fluctuations of dipolar chains

Serge Cutillas and Jing Liu

Department of Physics and Astronomy, California State University, Long Beach, California 90840

(Received 18 November 1999; published 25 June 2001)

Dynamic light scattering is used to study experimentally the dynamics of dipolar chains consisting of ferrofluid particles subjected to a magnetic field (H_0). The effective diffusion coefficient shows a pronounced dependence on the scattering wave vector q , reflecting two modes of motion: translational diffusion of the whole chain, and fluctuations of particles within a chain. The characteristic probed frequency of particle displacements is inversely proportional to H_0 , and exhibits a q^3 dependency. Based on the striking analogy to polymer chain dynamics, we attribute these behaviors to the contribution of hydrodynamic interactions (HI's) that couples particles motion within a chain. This work suggests that chain fluctuations cannot be ignored even for the very strong magnetic field applied (coupling constant $< 10^6$). HI's can still be important, even at an extremely low particle volume fraction of 10^{-5} .

DOI: 10.1103/PhysRevE.64.011506

PACS number(s): 47.50.+d

Electrorheological (ER) and magnetorheological (MR) suspensions show fascinating rheological properties: controlled by the applied field (electric or magnetic), the fluid changes from a liquid state to a solid state continuously and reversibly. This leads dipolar fluids to a wide range of applications in such diverse areas as mechanical engineering and medicine [1,2]. The reason for the rheological controllability is the formation of structures when the field is applied. In the case of a MR suspension, a magnetic dipole moment is induced in each particle by an applied magnetic field, creating dipole-dipole interactions between particles. This interaction is balanced by thermal motion. A coupling constant λ is used to describe the relative strength of these two energies [3]: $\lambda = \pi a^3 \chi^2 \mu_0 H_0^2 / 9kT$. Here a is the radius and χ the magnetic susceptibility of one particle, μ_0 is the vacuum permeability, H_0 is the effective magnetic field acting on each particle, and kT is the thermal energy. When λ is greater than 1, particles align into single chains parallel to the field direction. Subsequently, columns or other large structures can form by the lateral coalescence of chains [4]. Here we have defined λ the same way as de Gennes and Pincus first defined it [3]: λ is independent of the particle's local environment, and depends only on the particle magnetic properties and the external magnetic field, for dilute samples. The advantage of this definition is that once a field is applied, λ is known and does not vary with time, as it would if defined differently.

In spite of many studies in dipolar fluids that focus on rheological properties [1,5] and field-induced structural changes [1,4,6,7], the basic physics of column formation by lateral coalescence of single chains is still not clear. Two infinite straight chains do not attract unless they are almost in contact. Two finite chains repel, yet experiments show aggregation to columns. To explain this, Halsey and Toor (HT) proposed that chain fluctuations due to thermal energy induce a long-range attraction between chains, which causes lateral aggregation (similar to the London interaction) [8]. This long-range interaction is predicted to be independent of the applied field strength, and is strongest when the chain-chain separation is about the wavelength of chain fluctuations. Later, the HT model was modified to take into account field-dependent aggregation found in experiments [9] and

defect-driven coarsening [10,11]. There may be other causes for chain aggregation, such as a chain shift relative to its neighbor, and variable chain lengths among neighboring chains. However, it is still very interesting to know to what degree chain fluctuations affect the chain-chain interactions.

In this paper, we report on a dynamics study of single chains in a ferrofluid emulsion using dynamic light scattering (DLS). We have found that (1) chain fluctuations do exist even for short chains, and can only be neglected for extremely high magnetic field applied (~ 1 T). The chain motions consist of two parts: whole chain center-of-mass motion, and internal chain particle-position fluctuations. (2) The characteristic frequency probed by DLS, $\Omega(q)$, depends on the scattering wave vector as $\Omega(q) \sim q^3 a / \sqrt{\lambda}$. This suggests a contribution of hydrodynamic interactions (HI's) in the chain dynamics. The existence of HI's in a strongly interactive medium is not surprising. But it is surprising that we see it at a particle volume fraction as low as 10^{-5} , and for a magnetic interaction coupling constant as low as 17.

Video microscopy (VM) [12] was previously used to study single chain dynamics. Although the range of study is limited to two-dimensional and lower frequencies, VM obtained a similar dynamic behavior: $l \sim t^{1/3}$. Here l is the distance covered by a particle in a chain during time t . As noted by the authors, a dependency of $l \sim t^{1/4}$ should be expected *without* hydrodynamic interactions. Furst and Gast [14] also reported experiments on chain fluctuations measured by diffusing-wave spectroscopy. They showed that a discrepancy occurred between numerical simulations and experiments possibly due to HI's or magnetic interactions between chains for a semidilute suspension (a particle concentration of 1%) used in their experiment. Thus, from previous work, it is not clear that one needs to include HI's in ER and MR fluids.

To study chain dynamics, the advantages of using DLS vs VM are manifold: DLS covers a range of frequency ($\sim < 100$ MHz) much larger than that accessible to VM ($\sim < 10$ Hz), and DLS probes a three-dimensional sample volume rather than a two-dimensional sample volume with the volume much larger than that studied by VM. Even at a volume fraction as low as 10^{-5} , there are about 10^5 particles within

the scattering volume. Furthermore, due to our smaller particle diameter ($2a=0.46\ \mu\text{m}$), and lower particle density ($1.1\ \text{g/cm}^3$) of ferrofluid emulsion, diffusion dominates convection (Peclet number 0.02) so that sedimentation is not a problem on a time scale of an experiment ~ 30 min.

In this work, the ferrofluid emulsion consists of an aqueous suspension of kerosene-based ferrofluid droplets (particles) coated with a surfactant to prevent aggregation [15,16]. The relative, initial magnetic susceptibility of a ferrofluid droplet is equal to 1.22. The particle volume fraction is 10^{-5} to avoid both multiple scattering and chain-chain lateral aggregation. The particle radius a measured by DLS is $0.23\ \mu\text{m}$, with 7% of polydispersity. The emulsion sample is held in a test tube that is surrounded by an index match bath to reduce reflections and control the temperature. The sample holder is placed inside a pair of Helmholtz coils, as described in detail elsewhere [16]. A laser beam ($\lambda_0=514.5\ \text{nm}$) is focused to the sample by a lens, and the scattered light is collected at an angle θ by a single mode fiber, guided to a photomultiplier tube, and analyzed by a digital correlator. The scattering plane is perpendicular to the magnetic field direction. Therefore, this setup is only sensitive to particle and chain motions in the plane perpendicular to the field direction (motions normal to chain axis).

In self-beating mode, the intensity autocorrelation function measured by the correlator gives rise to the dynamic structure factor $S(q,t)$. In the absence of a magnetic field, the suspension is isotropic without any interactions between particles (very dilute sample). In this case, the dynamic structure factor reduces to a single exponential $S(q,t) \propto \exp(-q^2 D_0 t)$. $D_0=(kT/6\pi\eta a)$ is the diffusion coefficient of a single particle in a fluid of viscosity η . If interactions or particle size polydispersity cannot be ignored, we can still assume single exponential $S(q,t) \sim \exp(-q^2 D_{\text{eff}} t)$ at the short time limit [$t \ll (q^2 D_{\text{eff}})^{-1}$], where an effective diffusion coefficient D_{eff} is used to describe the particle or chain motion [17]. D_{eff} reduces to D_0 for monodisperse particles without interactions.

In the experiment, correlation functions are measured as a function of the applied magnetic field and the scattering angle θ which determines q through $q=4\pi n/\lambda_0 \sin(\theta/2)$. Here n is the refractive index of the water. q defines a characteristic length $l(=2\pi/q)$, and sets a window in which the motion of particles or chains is probed. Thus varying θ probes different length scales. If the chains are rigid, only one length scale is present in the scattering plane—the chain width. Therefore, the diffusion coefficient is q -independent. In this work, the scattering angle θ is varied between 5° and 130° . Thus, length scales are probed over the range of $0.9a < l < 20a$.

To study the scattering angle dependence, a magnetic field of 200 G ($\lambda=406$) is applied to the sample for 6 h to build separated chains first. The resulting chains have an average length of 19 particles, which is long enough to allow different motions to exist. The average chain separation is more than 70 particle diameters, which is far enough to slow down the chain growth substantially. Therefore, the chain length is almost constant during the next 30 min when the

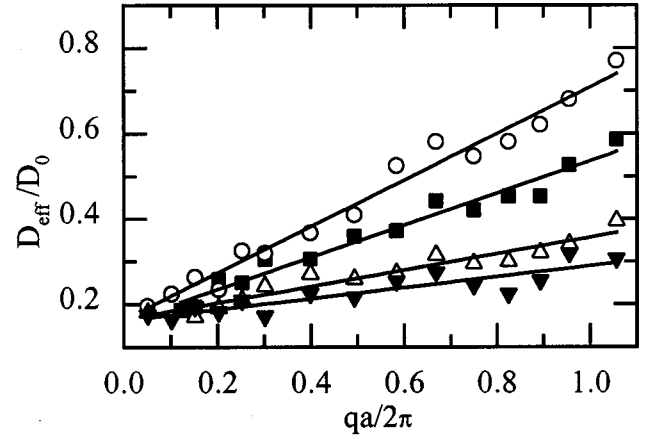


FIG. 1. Normalized effective diffusion coefficient vs the normalized scattering wave vector q for various applied magnetic fields (coupling constant λ). Solid triangle, $\lambda=406$; empty triangle, $\lambda=157$; square, $\lambda=46$; circle, $\lambda=17$. Solid lines are linear fittings.

angle-dependent DLS is performed [16]. We then vary the magnetic field strength (λ) and repeat the q -dependence experiment.

Figure 1 shows four experiments performed at different magnetic field or coupling constant λ where the average chain length was kept nearly equal. After the chain length was first established at $\lambda=406$, these four experiments were done in the order $\lambda=406, 17, 157, \text{ and } 46$. This order was chosen to minimize the chain growth and ensure an equal chain length during all four experiments, and at the same time to keep the coils from overheating. D_{eff} is normalized by D_0 . q is normalized by $2\pi/a$.

From Fig. 1, it is clear that D_{eff} depends on q , indicating additional motion other than rigid chain diffusion. The higher q is, the larger D_{eff} is. This additional motion becomes dominant when zoomed to a smaller length scale l . When l is much larger than the particle radius ($qa/2\pi \rightarrow 0$) DLS is mainly sensitive to the center of mass diffusion of the chain. Thus D_{eff} reflects the translational diffusion of the entire chain, which depends only on the number of particle per chain N and D_0 . In the opposite limit (i.e., $qa/2\pi \sim 1$), we are sensitive to motions on a length scale comparable to the size of individual particles. Here the main contributions to the measured diffusion coefficient come from internal motions of the chains (i.e., chain fluctuations). It is worth noting here that, using video microscopy under the same conditions as in the DLS experiments, we verified experimentally that no lateral aggregation occurred even for an average chain length longer than 100 particles. Furthermore, although chain breakage-reformation plays an important role in the chain formation at the thermodynamic equilibrium ($\lambda < 8$) [13], this does not happen in our case, as confirmed by our video microscopy observations. Thus the only physical mechanisms contributing to D_{eff} are the motions of the chain's center-of-mass and particle fluctuations within chains.

Figure 1 also shows that the slope of D_{eff} versus q increases as λ decreases. That is, internal fluctuations increase or the chain becomes less rigid for weaker magnetic interactions, as expected. Note that all the four straight lines con-

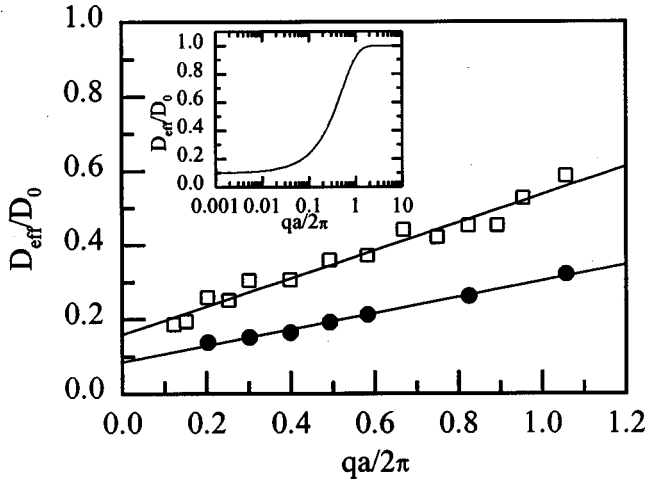


FIG. 2. Effect of different chain lengths on D_{eff} . Both data are taken at $\lambda=46$, while chains are first formed at $\lambda=406$ for three more hours for the data shown as solid circles than those shown as squares. Solid lines are linear fittings. The inset indicates the universal behavior of D_{eff} vs q in polymer physics.

verge to the same point ($D_{\text{eff}}/D_0=0.16\pm 0.01$) as q approaches zero. Since rigid chain motion is probed at low q , this convergence confirms the fact that the chain length is constant over the period of the four experiments, and the chains remain connected even for the lowest λ values used. As our earlier papers show, the transverse diffusion coefficient of a straight chain comprised of N particles is given by $D_{\text{chain}}=f(N)D_0$, where $f(N)=[3\ln(2N)+1.254]/4N$ [16,18]. Thus the average chain length can be calculated from the converging value of D_{eff} which gives $N=19\pm 1$.

From the slope of the four curves, the dependence of the diffusion coefficient on magnetic field is obtained. It shows a power-law relation $D_{\text{eff}}/D_0\propto\lambda^\delta$, with an exponent $\delta=-0.47\pm 0.05$. Thus D_{eff}/D_0 is approximately proportional to $1/\lambda$. Since $\lambda\sim H^2$ [3], D_{eff} is inversely proportional to the magnetic field. Therefore, D_{eff}/D_0 is experimentally found to take the following form:

$$D_{\text{eff}}/D_0\approx\frac{A}{\sqrt{\lambda}}g(N)qa+f(N). \quad (1)$$

Here A is a constant, and $g(N)$ is a function of N that needs to be determined. Equation (1) shows the two contributions to D_{eff} : fluctuations and translational motion of the whole chain.

$g(N)$ and A are determined by studying the effect of chain length on D_{eff} . To obtain a longer chain length than $N=19$, we hold the magnetic field at $\lambda=406$ for three more hours. We then reduce the field down to $\lambda=46$, and repeat the q -dependence measurements. The result is shown in Fig. 2. Here, when N varies, the initial value ($q\rightarrow 0$) is different. The slope is found to change as well. If we assume that $g(N)=N^\varepsilon$ in Eq. (1), then ε is found to be -0.7 ± 0.1 . Since $f(N)\approx\frac{3}{2}N^{-0.75}$ for $N>5$, $g(N)(=N^{-0.7})$ may be approximated by $\frac{2}{3}f(N)$. After $g(N)$ is known, the constant A is

found to be 3.0 ± 0.2 based on Eq. (1) and the data in Fig. 2. Thus putting the two approximations together, Eq. (1) becomes

$$D_{\text{eff}}\approx\left(\frac{2}{\sqrt{\lambda}}qa+1\right)D_{\text{chain}}. \quad (2)$$

Note that we can obtain Eq. (2) without any assumption about the chain size power-law dependency. Indeed, when plotting $D_{\text{eff}}/D_{\text{chain}}$ against qa , the data of Fig. 2 corresponding to $N=19$ and 42 collapse on a single straight line, with the slope equal to $2/\sqrt{\lambda}$ and the ordinate equal to 1, as shown by Eq. (2). From Eq. (2), D_{eff} , and thus the characteristic frequency of fluctuations from the dynamic structure factor, $\Omega(q)=q^2D_{\text{eff}}$ decrease when the chain length increases. This can be attributed to the longer wavelength and thus the slower fluctuating modes that dominate in longer chains. This chain length dependency of chain fluctuations cannot be explained by an increase of the local field acting on a particle inside a longer chain. Indeed, it is only for very short chains (<5 particles) or high magnetic susceptibilities ($\chi\gg 1$) that λ is sensitive to the chain length. Thus, for the same applied external magnetic field, λ should be the same for our experiments with the two chain sizes of 19 and 42 particles. Note that our experiments cover only a limited range of characteristic lengths $l(=2\pi/q)$. We are sensitive to the most interesting range of l where a q dependency of D_{eff} can be observed. However, if we could expand the q range toward 0 and ∞ , a different behavior of D_{eff} might be observed. In analogy to polymer dynamics [19,20], we expect a qualitative behavior, as shown in the inset of Fig. 2. Here three dynamic regimes exist. For small qa values, D_{eff}/D_0 corresponds to the diffusion of the entire polymer chain. In the opposite limit, $qa>2\pi$, D_{eff} asymptotically approaches the diffusion coefficient of monomers D_0 . In both limits, D_{eff}/D_0 does not depend on q . For dipolar chains, the expected constant regions in D_{eff} corresponding to these limits may be deduced from Eq. (2) by setting $qa=0$ and $qa=2\pi$ inside the brackets. When $qa=0$, $D_{\text{eff}}=D_{\text{chain}}$. The rigid chain motion is probed. When $qa=2\pi$, we assume that the maximum diffusion coefficient is obtained in Eq. (2).

The relative importance of internal fluctuations to whole chain diffusion is measured by the ratio of the two terms in Eq. (2) by setting $qa=2\pi$ to the maximum probed value of fluctuations: $D_{\text{flu}}/D_{\text{chain}}=4\pi/\sqrt{\lambda}$. At an extremely high field limit $\lambda\rightarrow\infty$, $D_{\text{flu}}=0$ and $D_{\text{eff}}=D_{\text{chain}}$. Chains become rigid, and the whole chain diffusion motion is probed. At the low field limit where $\lambda\gg 1$ to ensure chain formation [13], $D_{\text{flu}}/D_{\text{chain}}\leq 4\pi$. Therefore, the chain-fluctuation contribution can be an order of magnitude larger than the rigid chain diffusion during the equilibrium structure formation. It is thus possible that fluctuations cause chain coarsening in the first stages of the equilibrium structure formation, as Halsey and Toor suggested. Moreover, due to the square root dependence, even at our highest magnetic field ($\lambda=406$) internal fluctuations are still comparable (62%) to the chain diffusion. To reach $D_{\text{flu}}/D_{\text{chain}}<1\%$, λ has to be larger than 10^6 . In our case, even if saturation effects were disregarded, the

magnetic field would have to be 1 T to obtain completely rigid chains. Physically, this means that chain fluctuations cannot be neglected in almost all experiments composed of submicron superparamagnetic particles.

From Eq. (2), the characteristic frequency becomes

$$\Omega(q) \approx \left(\frac{2}{\sqrt{\lambda}} qa + 1 \right) q^2 D_{\text{chain}}. \quad (3)$$

This relation shows q^3 and $1/\sqrt{\lambda}$ dependencies. To understand this, we may compare the dipolar chains with polymer chains. In polymer physics, if only entropic spring forces (spring constant of $3kT/b^2$) are considered to connect the N monomers with their first neighbors, the chain motion is described by a set of N linearly coupled Langevin equations (Rouse model) [19,20]. This model predicts a characteristic frequency of $\Omega_{\text{Rouse}}(q) \sim q^4 b^2$. Here b is the effective bond length between two monomers. Conversely, if HI's couple the N Langevin equations in addition to besides the spring forces coupling, the Langevin equations become highly nonlinear. However, the Zimm model originally consisted of preaveraging the Oseen tensor to obtain analytic expressions resulting in a $\Omega_{\text{Zimm}}(q) \sim q^3 b$ dependency [19,20]. If dipolar interactions bind the particles in a chain (a spring constant of $3kT\lambda/a^2$), the Rouse model corresponds to $\Omega_{\text{Rouse}}(q) \sim q^4 a^2/\lambda$ (using $b^2 \equiv a^2/\lambda$), while the Zimm model corresponds to $\Omega_{\text{Zimm}}(q) \sim q^3 a/\sqrt{\lambda}$ in our case. Since both the q^3 and $a/\sqrt{\lambda}$ dependencies are shown in our measurements, this strongly suggests the influence of HI's on chain dynamics. The q^3 dependence is also observed in DNA molecules studied by DLS [21,22] showing that HI's affect the dynamics. As pointed out by de Gennes [19] in dynamic scaling arguments, it is general to find a q^3 behavior in the presence of HI's.

In the above comparison between dipolar chains and polymers dynamics, we need to clarify the following points. First, HI's do not come from interchain interactions, since our VM observations performed at the same conditions as in DLS experiments confirmed that only single chains were observed at this low volume fraction, and no chain coarsening occurred. Second, the spring constant we derived holds for transverse displacements (relative to its nearest neighbor) smaller than a particle diameter. Finally, the approximation made on nearest-neighbor interaction without magnetic induction may underestimate the absolute value of the spring constant by a factor of 2 at most, but not affect either the

$1/\sqrt{\lambda}$ or q^3 dependencies. Indeed, when particles gather, the internal magnetic field is no longer homogeneous within a particle, and is strongest at contact points where surrounding particles are located [23]. Since the magnetic susceptibility is a decreasing function of the internal field, the net magnetic susceptibility is reduced, limiting the effect of induction. Moreover, even in the absence of the magnetization saturation effect, the internal magnetic field is at most 68% higher for a homogeneous infinite cylinder than for a spherical particle made of the same ferrofluid as described above. This difference is reduced by the geometry of a chain of particles, a field-dependent magnetic susceptibility and a finite-size correction.

The existence of HI's is further supported by the data of previous work using VM [12] at a lower frequency range than ours. Although their simulation concluded differently, we believe that this is due to the discrepancy of λ used in the simulations and experiments. Therefore, the two experimental data over a large frequency range strongly suggest the influence of HI's on the single chain dynamics.

In conclusion, we find that, by varying the scattering wave vector, two separate modes of motion are resolved. One originates from the translational diffusion of the chain center of mass, and the other comes from particle fluctuations. As either the magnetic field or chain length increases, fluctuations decrease. However, chain fluctuations cannot be neglected in almost all experiments performed with submicron particles. At intermediate scattering wave vectors q , the characteristic probed frequency behaves as $\Omega(q) \sim q^3 a D_{\text{chain}}/\sqrt{\lambda}$. Both the q^3 and $1/\sqrt{\lambda}$ dependencies can be explained by considering the contribution of HI's according to the Zimm model developed in polymer dynamics. However, it remains open whether the origin of HI's is due mainly to nearest-neighbor motions or to whole chain diffusion that creates an additional random drag force on each particle. Although weak, coupling of sedimentation with diffusion may be another possible cause. An additional experiment performed with chain ends fixed could be used to clarify this point. Therefore, our experiments may serve as a first step to better understand HI's in complex fluids, since our particles (monomers) have a shape, a size, a separation, and interactions that are precisely controllable.

We gratefully acknowledge M. Hagenbüchle for initial work on dynamics studies and helpful discussion. This work was supported by a Grant from NASA (NAG 3-1830).

-
- [1] *Proceedings of the 5th International Conference on ER Fluids, MR Suspensions and Associated Technology, University of Sheffield, UK, July 1995*, edited by W. Bullough (World Scientific, Singapore, 1996).
- [2] R. Sheng, G. Flores, and J. Liu, *J. Magn. Magn. Mater.* **194**, 167 (1999).
- [3] P. G. de Gennes and P. A. Pincus, *Phys. Kondens. Mater.* **11**, 189 (1970).
- [4] J. Liu, E. M. Lawrence, A. Wu, M. L. Ivey, G. A. Flores, K. A.

- Javier, J. Bibette, and J. Richard, *Phys. Rev. Lett.* **74**, 2828 (1995).
- [5] E. Lemaire, A. Meunier, G. Bossis, J. Liu, D. Felt, P. Bashtovoi, and N. Matoussevitch, *J. Rheol.* **39**, 1011 (1995).
- [6] S. Cutillas, G. Bossis, and A. Cebers, *Phys. Rev. E* **57**, 804 (1998).
- [7] S. Cutillas and G. Bossis, *Europhys. Lett.* **40**, 465 (1997).
- [8] T. C. Halsey and W. Toor, *J. Stat. Phys.* **61**, 1257 (1990).
- [9] Y. Zhu, E. Haddadian, T. Mou, M. W. Gross, and Jing Liu,

- Phys. Rev. E **53**, 1753 (1996).
- [10] J. E. Martin, K. M. Hill, and C. P. Tigges, Phys. Rev. E **59**, 5676 (1999).
- [11] J. E. Martin, R. A. Anderson, and C. P. Tigges, J. Chem. Phys. **108**, 3765 (1998); **108**, 7887 (1998).
- [12] A. S. Silva, R. Bond, F. Plouraboué, and D. Wirtz, Phys. Rev. E **54**, 5502 (1996).
- [13] S. Cutillas, G. Bossis, E. Lemaire, A. Meunier, and A. Cebers, Int. J. Mod. Phys. B **13**, 1971 (1999).
- [14] E. M. Furst and A. P. Gast, Phys. Rev. E **58**, 3372 (1998).
- [15] J. Bibette, J. Magn. Magn. Mater. **122**, 37 (1993).
- [16] M. Hagenbüchle and J. Liu, Appl. Opt. **36**, 7664 (1997).
- [17] R. Klein, *Structure and Dynamics of Strongly Interacting Colloids and Supramolecular Aggregates in Solution*, Vol. 369 of *NATO Advanced Study Institute Series C: Structure and Dynamics of Strongly Interacting Colloids and Supramolecular Aggregates in Solution*, edited by S. Chen *et al.* (Kluwer, Dordrecht, 1992).
- [18] K. Zhan, R. Lenke, and G. Maret, J. Phys. II **4**, 555 (1994).
- [19] P. G. de Gennes, *Scaling Concepts in Polymer Physics* (Cornell University Press, Ithaca, NY, 1979).
- [20] A. Z. Akcasu, M. Benmouna, and C. C. Han, Polymer **21**, 866 (1980).
- [21] R. J. Lewis, S. A. Allison, D. Eden, and R. Pecora, J. Chem. Phys. **89**, 2490 (1988).
- [22] M. A. Ivanova, A. V. Arutyunyan, and A. V. Lomakin, Appl. Opt. **36**, 7657 (1997).
- [23] J. M. Ginder and L. C. Davis, Appl. Phys. Lett. **65**, 3410 (1994).